

Contribution of Surface Resonances to Scanning Tunneling Microscopy Images: (110) Surfaces of III-V Semiconductors

Ph. Ebert, B. Engels, P. Richard, K. Schroeder, S. Blügel, C. Domke, M. Heinrich, and K. Urban

Institut für Festkörperforschung, Forschungszentrum Jülich, D-52425 Jülich, Germany

(Received 12 October 1995)

We show that the conventional dangling bond picture is insufficient to explain scanning tunneling microscopy (STM) images of III-V (110) semiconductor surfaces. Voltage-dependent STM images combined with *ab initio* electronic structure calculations give evidence that surface resonances fundamentally change the STM images of InP, GaP, and GaAs (110). The occupied dangling bond state dominates the images at negative voltages, but its counterpart, the empty dangling bond state, is only of relevance for small positive voltages. The empty state images are rather governed by empty resonances which lead to a 90° rotation of the apparent rows. [S0031-9007(96)01271-9]

PACS numbers: 73.20.At, 71.10.-w, 71.15.Nc

The interpretation of topographic scanning tunneling microscopy (STM) images is straightforward as long as the structures of interest do not reach atomic scales. However, with the advent of increasingly smaller nanostructures, information within a surface unit cell or even smaller details around isolated features of subnanometer size become increasingly important. On this subnanometer scale the STM image is largely determined by the details of the surface electronic structure [1] and their interpretation becomes impossible without a theoretical background. Even today chemical sensitivity or the interpretation of details around impurity atoms, defects, and adsorbates remains largely impossible.

(110) surfaces of III-V semiconductors [2–4] provide a particularly interesting example for the interpretation of STM images on the basis of the electronic structure. In the past, these surfaces developed to model systems for the search of high-quality surface electrical contacts for materials with potential optoelectronic applications. The (110) surfaces can be obtained reproducibly by cleavage with a very low defect concentration [5] and a relatively simple (1 × 1) surface relaxation [6,7]. Indeed, the major effect of the surface relaxation consists of anions (e.g., P) relaxing outward relative to the cations (e.g., In) [8,9]. This relaxation drives the surface states out of the fundamental gap and results in one occupied and one empty dangling bond located at each anion and cation, respectively [10–12]. Consequently, the STM images should be easy to interpret, showing these dangling bonds, which can be correlated directly to the anion and cation sublattices [2].

On the other hand, some theoretical calculations [13,14] and photoemission data [15,16] show that all (110) surfaces of III-V compound semiconductors also have, in addition to dangling bond states, a variety of surface resonances [17]. Some of them are close enough to the band edges that they may contribute to the STM images. However, little is known about the nature of these resonances, and many experiments were analyzed without taking them into account [2,12]. In this Letter we demonstrate that the surface resonances change the STM image fundamentally.

The resonances are the origin of a 90° rotation of the apparent atom rows observed in high resolution STM images. Thus surface resonances veil the link between the topology of the STM tunnel current and the positions of the atoms, and pose a severe limitation on the understanding of adsorbates, point defects, and alloys.

In this Letter we compare high-resolution STM images for a large range of tunneling voltages to the lateral distribution of energy integrated local density of states obtained from self-consistent, *ab initio* electronic structure calculations in order to unravel the contributions of surface resonances to STM images. We found that images of the occupied states are dominated by the anionic dangling bond state, but the empty state images are mostly governed by surface resonances, not included in the simple dangling bond picture.

Experiments were performed using InP [Zn (1–2) × 10¹⁸ cm⁻³ and Sn (1–2) × 10¹⁸ cm⁻³], GaP [Zn (2–6) × 10¹⁷ cm⁻³ and S (5–6) × 10¹⁷ cm⁻³], and GaAs (Si 4 × 10¹⁸ cm⁻³) single crystals cleaved in ultrahigh vacuum. We measured high-resolution constant current images of the empty and occupied states at tunneling voltages ranging from -4.5 to +3 V (outside this range, the spectrum is dominated by barrier resonances or field emission resonances [17]). The imaging quality of the tip has been carefully tested, e.g., at step edges and vacancies to avoid double imaging effects, to give an exact vertical and an excellent lateral resolution. These images were then compared to electronic structure calculations based on the density functional theory in the local density approximation [18] combined with the plane wave pseudopotential technique [19,20]. A repeated slab model is used to simulate the semi-infinite surface problem. The structure optimization was obtained with a supercell containing a 9 layer slab separated by a vacuum region equivalent to 7 layers. Since typical surface resonances turned out to extend deep into the bulk, calculations of the electronic structure were repeated using a supercell with a slab of 17 layers of atoms in order to discriminate surface resonances from bulk states. The calculations are carried out with basis functions up to

a kinetic energy of 12 Ry and 4 k points in the irreducible wedge of the (110) surface Brillouin zone. We calculated the lateral variation r_{\parallel} of the local density of states (LDOS) $n(\mathbf{r}_{\parallel}, z|E)$ at several distances z from the surface. According to the approximation by Tersoff and Hamann [21], the variation of the tunneling current with bias voltage V is proportional to the LDOS of the sample at the tip position \mathbf{r}_0 , $dI/dV \propto n(\mathbf{r}_0|E_F + eV)$. Thus the energy integrated LDOS (ILDOS) of occupied ($V < 0$) or unoccupied ($V > 0$) states in the energy range $(E_F, E_F + eV)$ contribute to the tunneling current, $I(\mathbf{r}_0) \propto \int_{E_F}^{E_F + eV} n(\mathbf{r}_0|E) dE$, and can be directly compared with the contour map of constant current STM images. Hence, constant current STM images taken at different bias voltages provide information on the state resolved contribution to STM images.

A selection of the measured STM images taken at different bias voltages V is presented in Fig. 1. The panels (a)–(f) and (g)–(k) show the STM images for the empty and occupied states of GaP(110), InP(110), and GaAs(110), respectively. The STM images at small positive voltages (empty states) of all three surfaces show apparent atomic

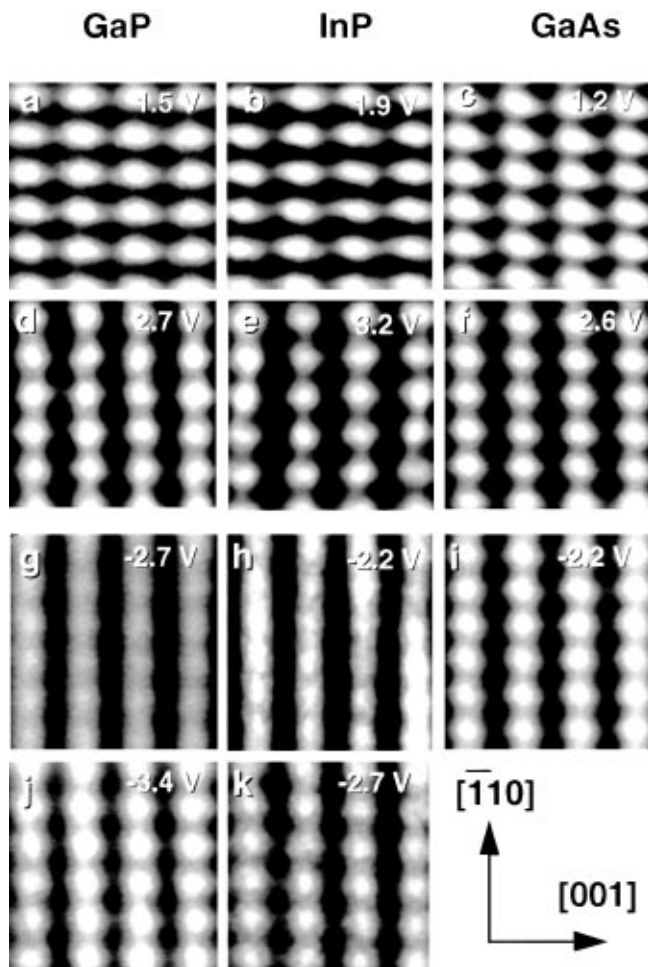


FIG. 1. Constant current STM images of the GaP, InP, and GaAs (110) surfaces measured at 0.4 nA tunneling current. The voltage of each frame is indicated in the right upper corner. (a)–(f) Empty states, and (g)–(k) occupied states.

rows aligned in the [001] direction [Figs. 1(a)–1(c)]. Towards higher voltages [Figs. 1(d)–1(f)] the apparent rows rotate by 90° and are thus oriented in the $[1\bar{1}0]$ direction. The STM images for negative voltages (occupied states) show no such change of the morphology. Only at higher negative voltages the resolution of the occupied states appears to be slightly better (even if the corrugation is smaller).

As a quantitative measure of the morphology changes in the STM images, we deduce the ratio of the atomic corrugation along the $[1\bar{1}0]$ and $[001]$ directions as a function of the voltage (Fig. 2). This choice eliminates many possible tip effects, since the ratio of corrugation does not depend on the absolute corrugation. Apparent atomic rows in the $[001]$ ($[1\bar{1}0]$) direction yield corrugation ratios larger (smaller) than one. The change of the corrugation ratio of the empty states is much larger than that of the occupied states. The corrugation ratio of the *empty states* decreases strongly with increasing voltage. But the position of the maximum of the empty LDOS is always above the cation, independent of voltage. In contrast, the corrugation ratio of the *occupied surface states* increases only slightly from -3 to -3.5 V. This arises from a decrease of the corrugation along the $[001]$ direction, while no changes are observed in the $[1\bar{1}0]$ direction.

We observed the same changes of the corrugation with different high resolution tips independent of the doping of the samples. From n - to p -doped surfaces only the voltage scale is slightly shifted, due to a different tip-induced band bending. Similarly, the absolute voltage at which the corrugation changes is slightly tip dependent, but not the effect itself. No significant differences are observed between InP, GaP, and GaAs (110) surfaces.

In order to understand the origin of these voltage-dependent morphology changes, we made a detailed analysis of the electronic structure for the InP(110) surface.

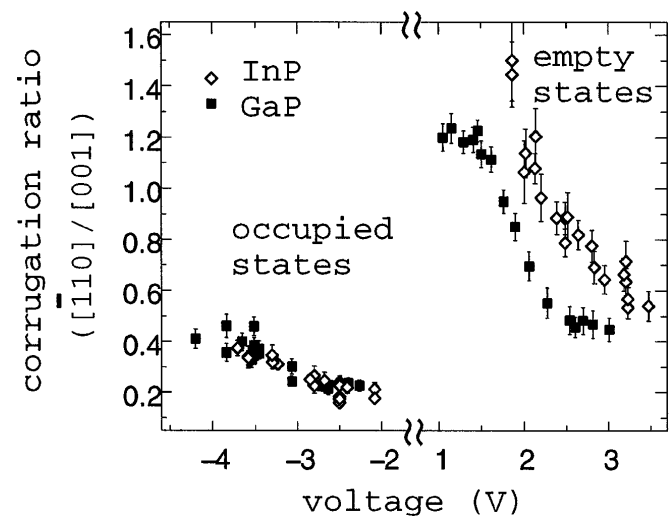


FIG. 2. Corrugation ratios for GaP and InP deduced from the STM images. The empty (occupied) states refer to n (p)-doped samples.

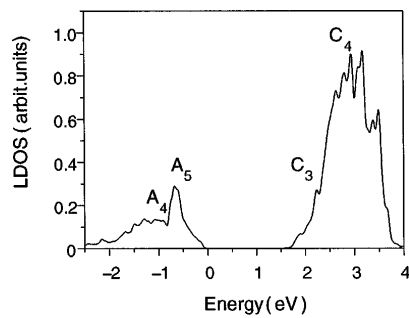


FIG. 3. Calculated LDOS $n(z_0|E)$, integrated over r_{\parallel} of the surface unit cell at a distance of $z_0 = 0.36$ nm from surface, measured from the outwardly relaxed P atoms. The origin of the energy scale is positioned arbitrarily at the valence band maximum. Four features are distinguished, marked with A_4 , A_5 , C_3 , and C_4 .

Figure 3 shows the laterally averaged computed LDOS at a distance of 0.36 nm from the surface. Four different surface states and resonances can be distinguished, marked by A_4 , A_5 , C_3 , C_4 using the same notation as in Ref. [13]. For each of these states the spatial distribution of the charge density of a typical representative wave function is shown in Fig. 4. The A_5 and A_4 states have charge densities localized at the anion. The A_5 state corresponds to the occupied dangling bond state. The occupied resonance A_4 is predominantly a back bond state with some small contributions from the rehybridization with bulk states. The C_3 state has all the charge density located at the cation and corresponds to the empty dangling bond state. Of particular interest is the empty resonance C_4 , which has a sizable contribution located in the surface above the cation as well as the anion.

All four features can contribute to the tunneling current. As discussed above, the tunneling current at a given bias voltage is proportional to an energy integral of the LDOS. Figure 5 shows contour plots of the LDOS integrated over energy intervals characteristic for the four different states.

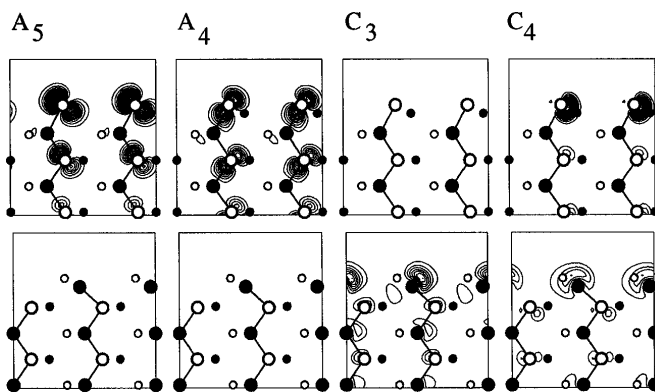


FIG. 4. Charge densities $|\psi_{k\nu}(r)|^2$ at characteristic states ($k\nu$) for the four identified features of the LDOS: A_4 , A_5 , C_3 , C_4 . All panels show $(1\bar{1}0)$ planes, cut perpendicular to the (110) surface. The upper panels show the $(1\bar{1}0)$ planes through the surface P atoms (anions), while the lower panels represent planes through the surface In atoms (cations).

Added are the sums of the ILDOS for the two occupied and empty states, which should correspond to STM images measured at large negative and positive tunneling voltages. At small negative voltages only the occupied dangling bond A_5 is imaged. With increasing voltage the STM will image increasingly more of the occupied resonance A_4 . However, the ILDOS of the resonance is smaller than that of the dangling bond state. Thus, at large negative voltages the images $A_4 + A_5$ will remain being dominated by the dangling bond state. This situation is completely different for the empty states. The empty dangling bond C_3 is only imaged at very small positive voltages. The most striking feature in Fig. 5 is the rotation of the apparent rows with increasing contribution of the empty resonance C_4 for positive voltages. Since the ILDOS of C_4 is much higher than that of the empty dangling bond, the resonance dominates the empty state STM images $C_3 + C_4$. This agrees very well with the STM images in Fig. 1. This rotation of the apparent row direction is due to the partly anionic character of the C_4 state. As discussed before, the state C_4 has a LDOS localized at the anion and at the cation. From this one would naively expect to find a zigzag chain in the STM image, which is actually predicted by ILDOS contour plots very close to the surface.

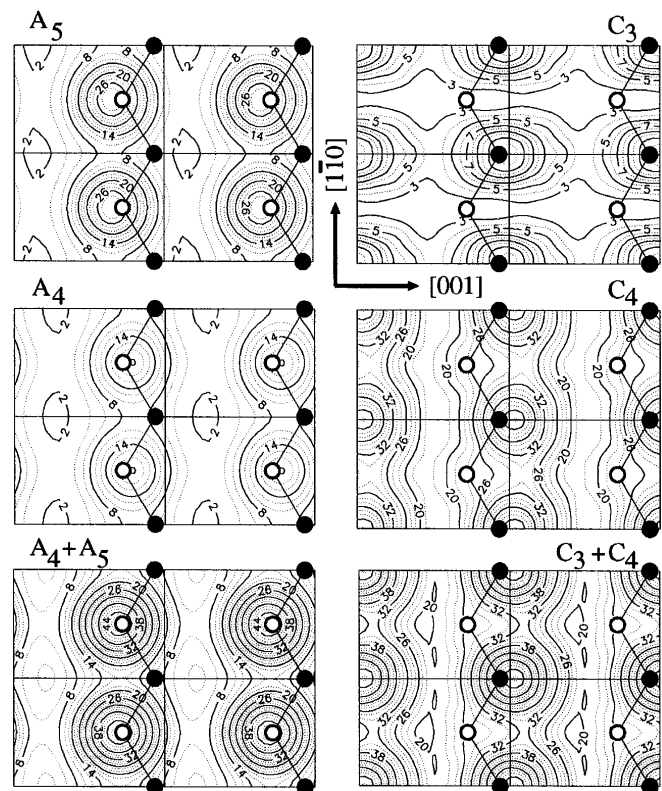


FIG. 5. Calculated lateral distribution r_{\parallel} of the ILDOS $\int n(r_{\parallel}, z_0|E) dE$ at a distance of $z_0 = 0.36$ nm from the surface, measured from the outwardly relaxed P atoms. The panels show integrals over different energy ranges characteristic for the different states: A_5 : -0.95 to 0 eV, A_4 : -1.77 to -0.95 eV, $A_4 + A_5$: -1.77 to 0 eV, C_3 : 0 to 2.27 eV, C_4 : 2.27 to 2.81 eV, $C_3 + C_4$: 0 to 2.81 eV.

However, the LDOS above the anion decays faster into the vacuum than above the cation, thus leaving a state C_4 with a reduced anionic character, rotating the apparent row direction rather than showing a zigzag chain. An overall quantitative agreement between theory and experiments has been obtained. In agreement with the experiment a corrugation ratio of about 1.1 and 0.6 was calculated from the ILDOS of state C_3 and $C_3 + C_4$. For the occupied states only a slight shift of the position of the maximum current is observed also agreeing with the STM images. Our results show that the difference between the occupied and empty states is not due to an equal empty vacuum charge on anions and cations as suggested previously [22] but rather due to the contribution of resonances.

Despite the overall agreement the voltage scales of experiment and theory do not coincide. This can be explained by band bending effects. As is well known, only for highly conductive surfaces and clean metallic tips, the voltage V applied to the sample corresponds directly to the energy eV used in the calculation. For all other cases, there is a tip-induced band bending at the surface and even at the tip, and an effective charging of the surface due to the high current density. The band bending reduces the effectively applied voltage and thus limits the true energy range reachable. From a comparison of the theoretical and experimental voltage ranges we estimate the band bendings at the border A_4/A_5 and C_3/C_4 to be about -2 eV for negative voltages (p -type samples) and $+0.5$ eV for positive voltages (n -type), respectively, which agree well with the calculated ones in Ref. [23].

Recently, Feenstra presented tunneling spectra for a variety of direct gap III-V semiconductors [24]. The energies of the identified surface states coincide well with the calculated ones. For those measurement conditions, Feenstra showed that the band bending is nearly negligible, different from our work. The difference can be explained by our lower doping concentration (2×10^{17} to 3×10^{18} cm^{-3} instead of 0.9×10^{19} to 5×10^{19} in Ref. [24]) and significantly different tip and measurement conditions [25].

In conclusion, by combining scanning tunneling microscopy experiments and self-consistent, *ab initio* electronic structure calculations, we presented evidence that surface resonances make vital contributions to STM images of (110) surfaces of III-V compound semiconductors. The spatial distribution of the LDOS of these resonances differ from those of the classic dangling bond states. This changes the relationship between the morphology observed in STM images and the atomic arrangement and causes, for instance, in the case of the III-V semiconductors a 90° rotation of the apparent atom rows. The comparison between theory and experiment reveals that the occupied dangling bond state dominates the images for negative voltages, but its counterpart, the empty dangling bond state, makes only minor contributions to the empty state STM images, sig-

nificant only for small positive voltages. The empty state images at larger positive voltages are dominated by empty surface resonances, which extend far out into the vacuum. The empty resonance has a sizable LDOS on the anion, although it is mainly cationic. We found that the classic dangling bond picture is a reasonable approximation for the occupied states, but fails to explain the empty states.

-
- [1] J. A. Stroscio, R. M. Feenstra, and A. P. Fein, Phys. Rev. Lett. **57**, 2579 (1986).
 - [2] R. M. Feenstra, J. A. Stroscio, J. Tersoff, and A. P. Fein, Phys. Rev. Lett. **58**, 1192 (1987).
 - [3] L. J. Whitman, J. A. Stroscio, R. A. Dragoset, and R. J. Celotta, Phys. Rev. Lett. **66**, 1338 (1991).
 - [4] Ph. Ebert, M. G. Lagally, and K. Urban, Phys. Rev. Lett. **70**, 1437 (1993).
 - [5] Ph. Ebert, *et al.*, Phys. Rev. B **51**, 9696 (1995).
 - [6] P. Mark, S. C. Chang, W. F. Creighton, and B. W. Lee, Crit. Rev. Solid State Sci. **5**, 189 (1975).
 - [7] D. J. Chadi, Phys. Rev. B **19**, 2074 (1979).
 - [8] A. R. Lubinsky, C. B. Duke, B. W. Lee, and P. Mark, Phys. Rev. Lett. **36**, 1058 (1976).
 - [9] A. Kahn, Surf. Sci. **168**, 1 (1986).
 - [10] S. Y. Tong, W. N. Mei, and G. Xu, J. Vac. Sci. Technol. B **2**, 393 (1984).
 - [11] J. L. A. Alves, J. Hebenstreit, and M. Scheffler, Phys. Rev. B **44**, 6188 (1991).
 - [12] H. Carstensen, R. Claessen, R. Manzke, and M. Skibowski, Phys. Rev. B **41**, 9880 (1990).
 - [13] J. R. Chelikowsky and M. L. Cohen, Phys. Rev. B **20**, 4150 (1979).
 - [14] F. Manghi, C. M. Bertoni, C. Calandra, and E. Molinari, Phys. Rev. B **24**, 6029 (1981).
 - [15] A. Huijser, J. van Laar, and T. L. van Rooy, Phys. Lett. **65A**, 337 (1978).
 - [16] L. Sorba, V. Hinkel, H. U. Middelman, and K. Horn, Phys. Rev. B **36**, 8075 (1987).
 - [17] The surface resonance is a particular type of surface state, which hybridizes with bulk states, but maintains a high density of states at the surface. It should not be confused with tip-induced field emission resonances at bias voltages larger than the work function. See, e.g., G. Binnig *et al.*, Phys. Rev. Lett. **55**, 991 (1985).
 - [18] S. H. Vosko, L. Wilk, and M. Nusair, Can. J. Phys. **58**, 1200 (1980).
 - [19] J. Ihm, A. Zunger, and M. L. Cohen, J. Phys. C **12**, 4409 (1979).
 - [20] P. Richard, B. Engels, K. Schroeder, and S. Blügel (to be published).
 - [21] J. Tersoff and D. R. Hamann, Phys. Rev. Lett. **50**, 1998 (1983).
 - [22] J. Tersoff and D. R. Hamann, Phys. Rev. B **31**, 805 (1985).
 - [23] J. A. Stroscio and R. M. Feenstra, J. Vac. Sci. Technol. **5**, 923 (1987).
 - [24] R. M. Feenstra, Phys. Rev. B **50**, 4561 (1994).
 - [25] R. M. Feenstra (private communication).